The topography of the mantle seismic discontinuities beneath the Alaskan subduction zone

Annemijn van Stiphout[1], Sanne Cottaar[2], Arwen Deuss[1]

[1]Faculty of Geosciences, Utrecht University, the Netherlands (a.m.vanstiphout@uu.nl)

[2]Department of Earth Sciences, University of Cambridge, United Kingdom

Questions? Ask Annemijn

1. Introduction

In the Alaskan subduction zone, the Pacific plate subducts underneath the North American Plate. Different seismic tomographic models do not agree on the depth extent of the slab. Here, receiver function analysis is used to study the topography of the global mantle discontinuities, to gain more insight in the Earth structure underneath Alaska. This research has been possible by the recent deployment of the USArray Transportable Array (TA) stations.

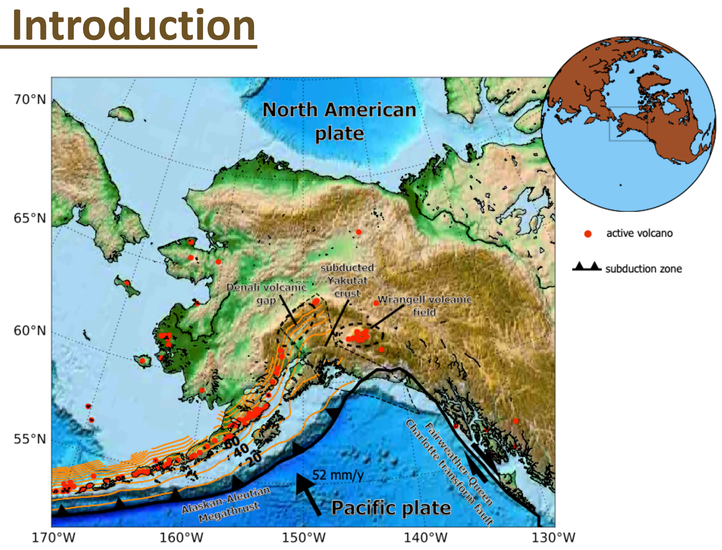

Figure 1: Map with the geometry of the Alaskan subduction zone. The orange lines show the subducted Pacific plate at depth with contour intervals of 20 km (Hayes et al. 2012) .

2. Seismic discontinuities

- The globally observed major seismic velocity discontinuities around depths of 410 and 660 km mark the top and the bottom of the mantle transition zone, the region that divides Earth's upper and lower mantle
- These discontinuities have been interpreted as polymorphic phase changes in the olivine system
- The phase transitions do not occur at the exact same depth everywhere, but vary depending on temperature, composition and water content
- For example, in colder regions like a subducting slab, an uplifted 410 and depressed 660, and thus a thicker mantle transition zone, are expected

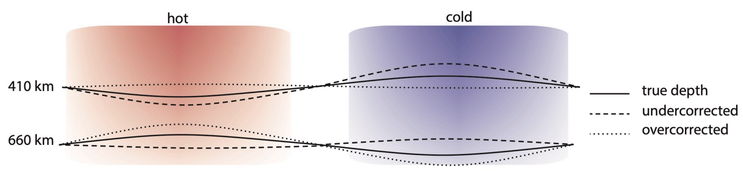

Figure 5: Cartoon showing the implications of velocity anomalies in the upper mantle and MTZ for the discontinuity depths. The topographies on the discontinuities are exaggerated.

3. Methods

- Receiver functions use the fact that P to S conversion takes place when a seismic ray hits a discontinuity
- P660s and P410s have travelled as P-wave first, and only a small part as S-wave
- They arrive 40 to 70 seconds after the direct P-arrival

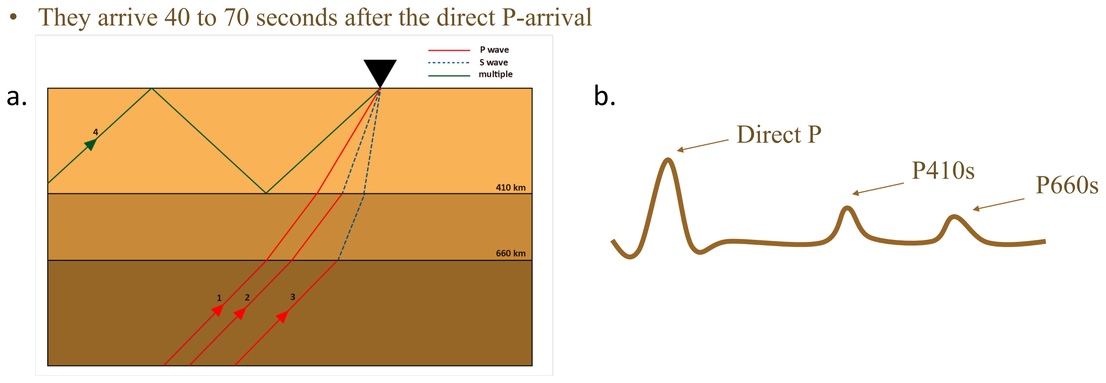

Figure 2: (a) Ray paths of a direct P-wave (1), the two converted phases P410s (2) and P660s (3) and a multiple (4). (b) Example of a receiver function. The direct P and two converted phases are indicated.

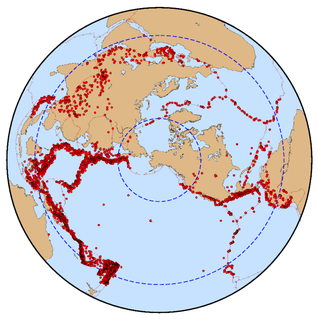

Figure 3: Distribution of events from 2000-2018 with Mw between 5.5 and 8.3, used in this study, shown with red circles, The blue contours define the epicentral distance range of 30˚ to 90˚ from the centre of Alaska. The final data set before quality control consists of 405,348 event to station pairs from 477 stations across Alaska.

- After quality check 27,800 radial receiver functions are used to make a common conversion point stack
- Regional velocity anomalies are accounted for by two regional tomographic velocity models by (1) Martin-Short et al. (2018), hereafter MABPM, and (2) Jiang et al. (2018), hereafter JSWLW

Large fast velocity anomaly: the subducting Alaskan slab

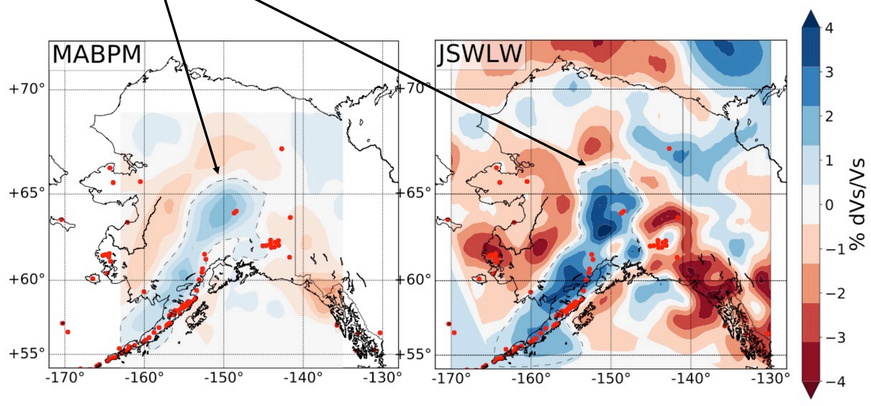

Figure 4: Shear wave velocity variations at 390 km depth for the 3D velocity models MABPM and JSWLW used for the time to depth correction. The large fast velocity anomaly is interpreted as the subducting Alaskan slab, indicated by the grey dashed line. Active volcanoes at the surface are plotted in red. Note the large amplitude difference between the models.

References and Acknowledgements

Dziewonski, A. M. and Anderson, D. L. (1981). Preliminary reference Earth model. Physics of the earth and planetary interiors, 25(4):297–356

Hayes, G. P., Wald, D. J., and Johnson, R. L. (2012). Slab1.0: A three-dimensional model of global subduction zone geometries. Journal of Geophysical Research: Solid Earth, 117(B1).

Jiang, C., Schmandt, B., Ward, K. M., Lin, F.-C., and Worthington, L. L. (2018). Upper mantle seismic structure of Alaska from Rayleigh and S wave tomography. Geophysical Research Letters, 45(19):10–350.

Martin-Short, R., Allen, R., Bastow, I. D., Porritt, R. W., and Miller, M. S. (2018). Seismic imaging of the Alaska subduction zone: Implications for slab geometry and volcanism. Geochemistry, Geophysics, Geosystems.

This project has received funding from the European Research Council (ERC) under the European Union's Horizon 2020 research and innovation programme (grant agreement No 681535 - ATUNE) and a Vici award number 016.160.310/526 from the Netherlands organization for scientific research (NWO). The facilities of IRIS Data Services, and specifically the IRIS Data Management Center, were used for access to waveforms, related metadata, and/or derived products used in this study.

4. Results & Discussion

Before rescaling

- The depth of the discontinuities is very dependent on the velocity model used for the mantle corrections
- The strong differences between the topography obtained by the two models are due to the large amplitude differences in the tomographic models

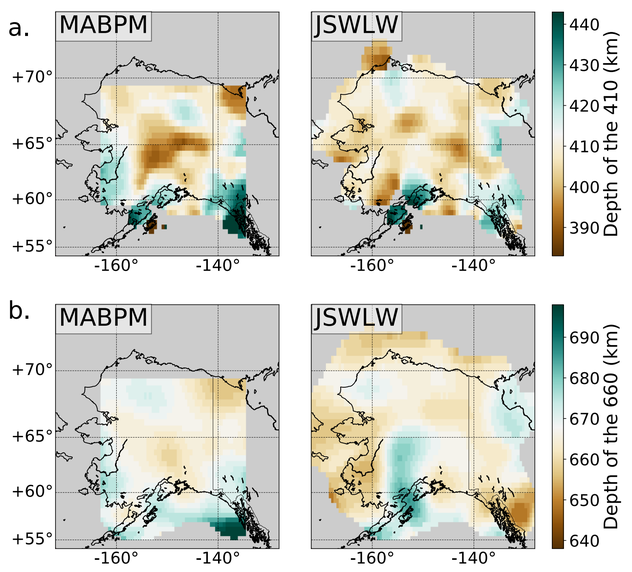

Figure 6: Depth of the peak amplitudes in the receiver functions corresponding to (a) the depth of the 410 discontinuity and (b) the depth of the 660 discontinuity for the original MABPM and JSWLW velocity models. Results are plotted if the sum of weights for the CCP stack is more than 40 stacked receiver functions and if the arrivals are significant.

- We show in figure 7 that correlations between the depth of the discontinuities and the topographic corrections from the 3D velocity model can be used to test the degree of under- or over-correction
- We found one model under-corrected and the other model over-corrected, and rescaled the topographic corrections to obtain comparable topographic maps

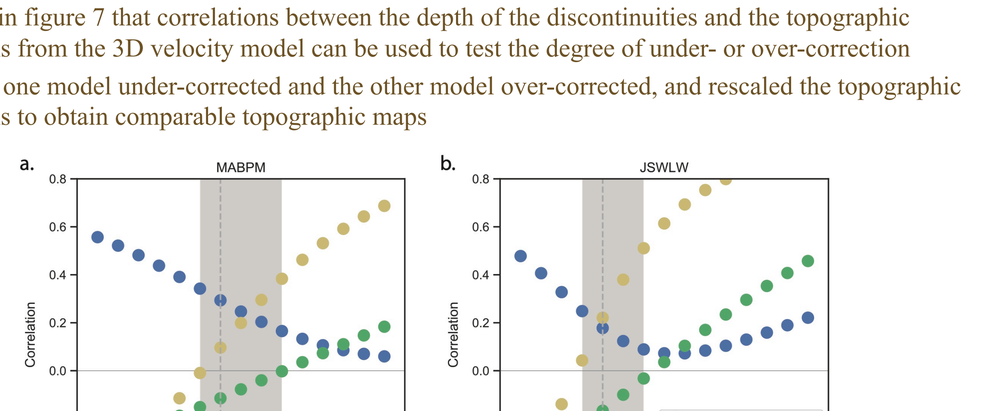

Figure 7: Correlations with different rescaling factors for (a) model MABPM and (b) model JSWLW. Factors are multiplied with the difference between the topography of the 3D model and PREM (Dziewonski and Anderson, 1981) and added to the PREM topography. Models get stronger with factors larger than zero, and less strong with factor smaller than zero.

Slab signature

After rescaling

- The topography maps look more similar
- We have successfully imaged the slab at 410 km depth and shown that it has clearly penetrated into the mantle transition zone
- Less variation on the 660, indicating the slab ends somewhere in the transition zone
- A thinner than normal transition zone is observed in the southeast, which may be caused by hot mantle upwellings associated with a slab window

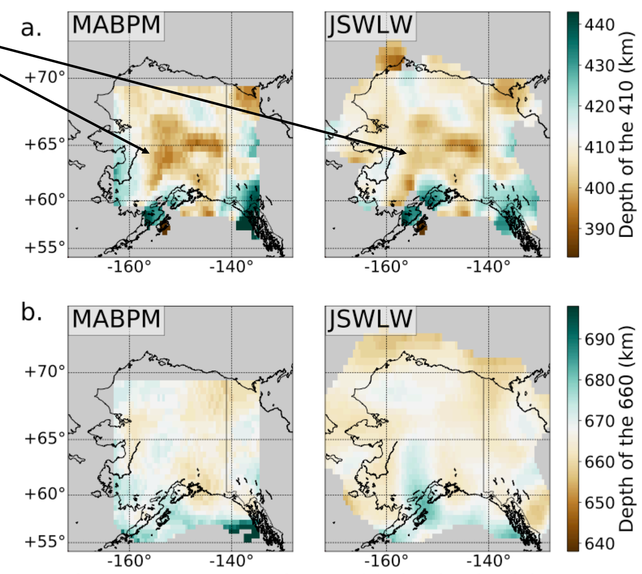

Figure 8: Depth of the peak amplitudes in the receiver functions corresponding to (a) the depth of the 410 discontinuity and (b) the depth of the 660 discontinuity for the rescaled MABPM and JSWLW velocity models. Results are plotted in the same way as in figure 6.